Introduction

NMR spectroscopy is a powerful tool for the accurate 3D-structural elucidation of the organic molecules, natural products and bio-molecules. However, resolution and sensitivity are major concern in NMR spectroscopy. Importantly, chemical shifts, *J*-couplings and NOEs are the key structural parameters in ^{1}H-NMR based structural elucidation of molecules, and precise determination of these parameters is vital for the accurate structural elucidation. Nevertheless, extraction of the valuable structural information is often hampered by signal overlap, primarily because of ^{1}H–^{1}H scalar coupling multiplets crowded over an inherently limited ^{1}H chemical shift range (~10 ppm), even at typical high magnetic fields. The problem of spectral resolution is more acute for the samples with complex spectral patterns. The sensitivity gains provided by the higher magnetic fields and advanced cryo probe technology partially circumvent the sensitivity issues for many applications. Resolution is magnetic field dependent, and it could be enhanced only by a factor 2 (from 500 MHz to 1000 MHz) over the 30 years (from 1980 to 2010). Therefore, there is a need for techniques to improve the resolution of NMR spectra, particularly for ^{1}H NMR and homonuclear correlation experiments in general. The spectral resolution further degrades in solid-state samples due to the dipolar and chemical shift anisotropy (CSA)-dominated line broadening, even under the magic angle spinning (MAS).

In order to address these issues, the present ***Thesis*** is focused on the development of advanced spectral simplification methods in both solution and solid-state NMR and the methods have been demonstrated for organic molecules, complex mixtures and unnatural cyclic peptides that mimic Amyloid type aggregation. Further, the work has been extended to explore morphology of liquid crystalline phases by using ^{129}Xe NMR spectroscopy, which is very sensitive to the local environment and does not involve painstaking ^{2}H labelling. Accordingly, the ^{129}Xe NMR of dissolved xenon gas in liquid crystal reports the physical parameters of its local environment and their variations with respect to external stimuli like temperature and macroscopic order parameter.

Chapter-1 provides a general introduction to the advanced NMR spectroscopic methods and their applications to resolve complex systems.

Chapter-2 discusses about novel 2D band-selective excited (BSE) PSYCHE-TOCSY method and its applications.

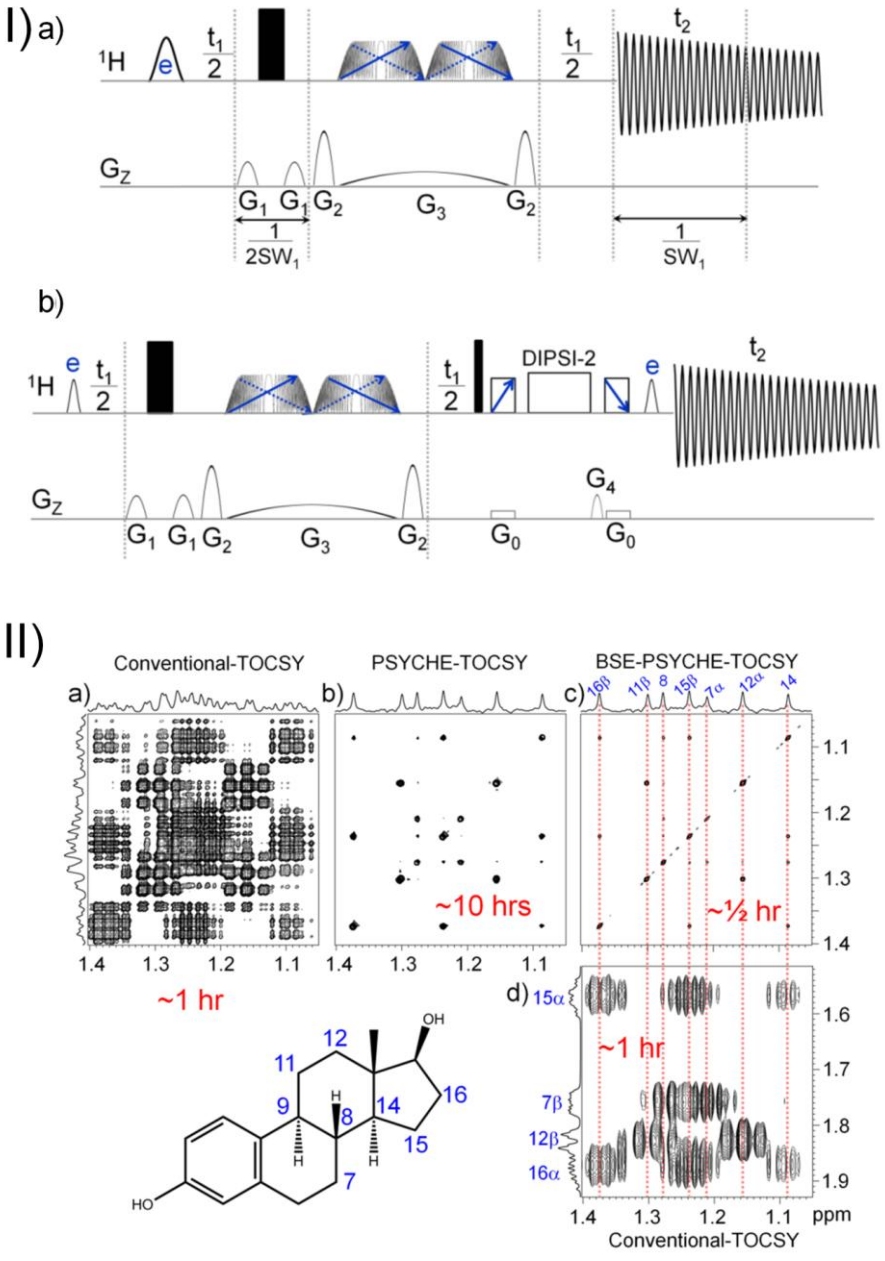

Figure 1: I) Pulse sequences for 1D BSE-PSYCHE (a) and 2D BSE-PSYCHE-TOCSY (b). II) Comparison of expanded regions of conventional 2D TOCSY (a and d), 2D full-band PSYCHE-TOCSY (b) and 2D-BSE-PSYCHE-TOCSY (c) spectra of Estradiol in DMSO-D_6.

Precise assignments of ^{1}H atomic sites and establishment of their through-bond COSY or TOCSY connectivity are crucial for molecular structural characterization by using ^{1}H NMR spectroscopy. However, this exercise is often hampered by signal overlap, primarily because of ^{1}H–^{1}H scalar coupling multiplets, even at typical high magnetic fields. In order to circumvent this issue, the present chapter describes a fast homonuclear band-selective ultrahigh resolution pure-shift TOCSY pulse sequence, BSE-PSYCHE-TOCSY, which is achieved through band-selective excitation followed by broadband PSYCHE homodecoupling along the indirect dimension. The significant advantages with this approach are the following: (i) drastic reduction in the experimental times (a factor from 10 to 20) compared with its broadband analog and (ii) complete broadband decoupling within excited band of choice, thereby offers enhanced resolution over the earlier HOBS decoupling. The pulse scheme is particularly helpful for quick screening of molecules or establishing through-bond connectivities. The efficacy of the BSE-PSYCHE-TOCSY has been experimentally demonstrated for two different intricate systems, Estradiol and a complex carbohydrate mixture. The method may potentially be extended to complex organic molecules of low concentrations or solubility and to metabonomics.

Chapter-3: Unambiguous ^{1}H-chemical-shift assignments and $^{n}J_{HH}$ scalar coupling values serve as essential inputs for precise structural elucidation of molecules in ^{1}H-based 2D-NMR spectroscopy. However, this important structural information is often obscured due to the inherent poor resolution of ^{1}H NMR spectra, that is mainly caused by the overlapping *J*-multiplets. By ^{1}H-^{1}H homodecoupling, the scalar multiplets suppress into nice singlets, thereby enhance resolution/spectral simplification. However, the rich structural information such as local configuration/conformation provided by scalar couplings is lost. Therefore it would be ideal to have both pure-shift as well as *J*-coupling information simultaneously. In principle, conventional 2D *J*-resolved NMR methods reported earlier should address this problem. However, the earlier methods could not effectively separate the scalar couplings and chemical shifts into two different dimensions, particularly for complex molecules. In order to circumvent this problem, two new two-dimensional (2D) *J*-resolved pure-shift NMR pulse sequences: ZFSE-PSYCHE and its selective excitation/refocusing version, SR-ZFSE-PSYCHE, that rely on the Morris's broadband homodecoupling element PSYCHE, have been reported.

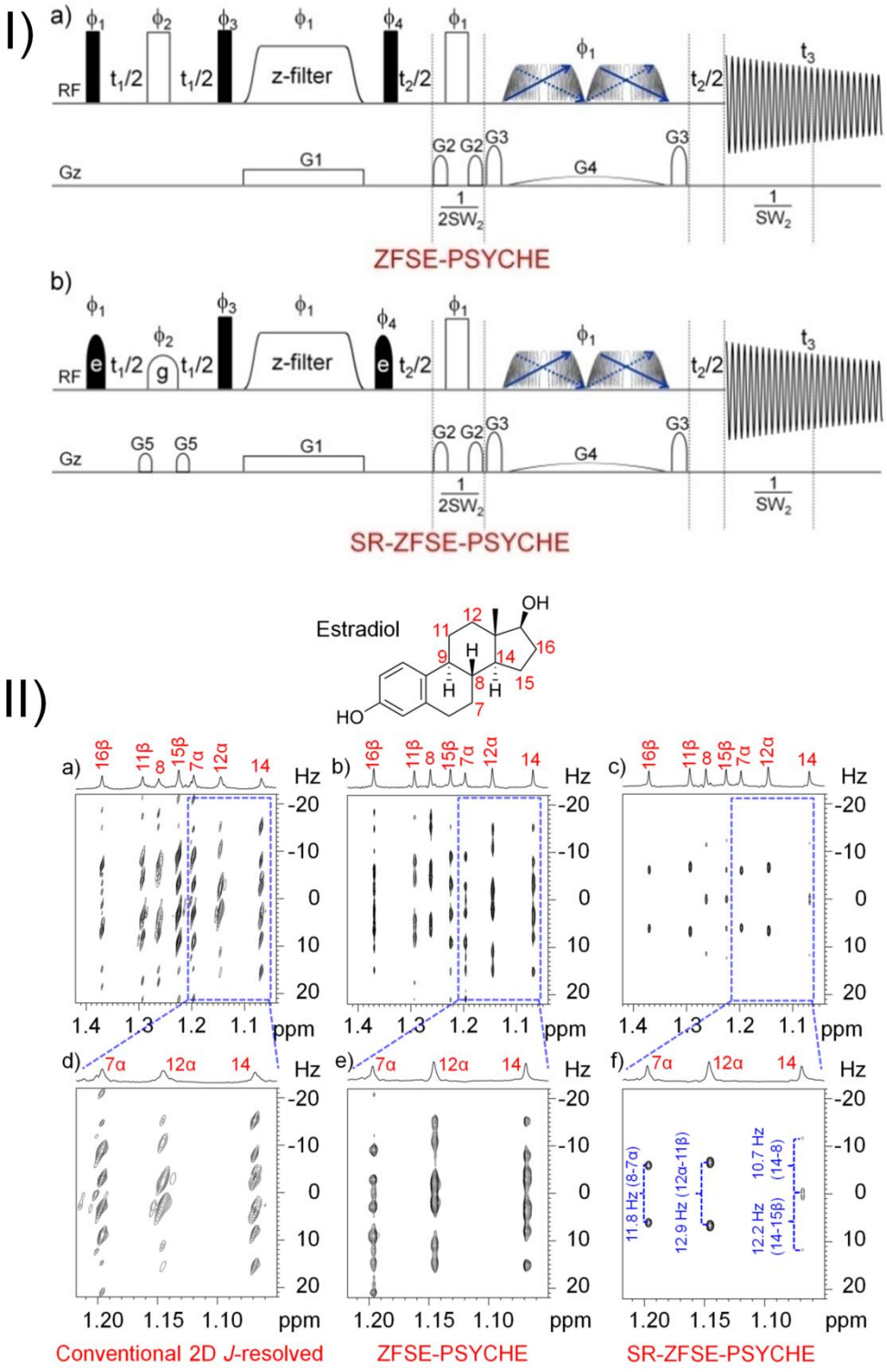

Figure 2: I) Pulse sequences for ZFSE-PSYCHE (a) and SR-ZFSE-PSYCHE (b) 2D *J*-resolved spectroscopy. II) Comparison of expanded regions of conventional (a and d), ZFSE-PSYCHE (b and e) and SR-ZFSE-PSYCHE (c and f) 2D *J*-resolved spectra of Estradiol in DMSO-D_6.

Unlike the conventional 2D *J*-spectroscopy methods, the ZFSE-PSYCHE and SR-ZFSE-PSYCHE facilitate information on local configuration/conformation through clearly resolved *J*-multiplets on F1-dimension as well as explicit identification of the corresponding ^{1}H sites through the multiplet-free pure-shifts, on the F2-dimension of the same 2D-spectrum. Results show that the full band 2D-*J* PSYCHE spectra alone can't completely resolve the structural/spectral complexities, which, however, should be substantiated by the corresponding band-selective excitation/refocused SR-ZFSE-PSYCHE experiments. Overall, despite the ZFSE-PSYCHE and SR-ZFSE-PSYCHE are time consuming pseudo-3D experiments, they serve as powerful and versatile broadband homodecoupling methods for the structural analysis of complex synthetic/natural organic molecules.

Chapter-4: In order to gain insight into the bio-molecular self-assembly processes involved Amyloid peptides such as ^{306}VQIVYK^{311}, and to propose plausible inhibitors, newer peptide scaffolds as models are constantly reported. Solid-state NMR plays an important role in gaining structural insights of these self-assembled structures. In this connection, the present chapter describes the design, synthesis, and solid-state NMR/DFT characterization of a new class of uniformly ^{13}C, ^{15}N-labelled unnatural peptides that self-assemble as needle-like structures and their synthetically modified analogs as inhibitors. A solid-state NMR method: i) off-magic angle spinning (Off-MAS), ii) selective spin-echos and iii) multiple-quantum filtering, is employed for the estimation of selective ^{13}C-^{13}C internuclear dipolar couplings in self-assembled cyclic-*β*-ASAS-tetrapeptide. The inter-nuclear distances of δ_{13C}-δ_{13C} (~5.6 Å) and β_{13C}-β_{13C} (~5.4 Å) thus derived for adjacent rings are in agreement with those calculated by DFT. Herein, Hadamard solid-state NMR methods developed in our laboratory are also explored. Density functional theory calculated structures have shown that the favorable β-sheet interaction of the N-methylated cyclic tetrapeptide with VQIVYK is mediated through intermolecular hydrogen bonding. The other face of the cyclic tetrapeptide with backbone N-methylation block the fibril growth hydrogen bonding edge and prevents from addition of another β-strand of VQIVYK, thereby inhibit the further aggregation.

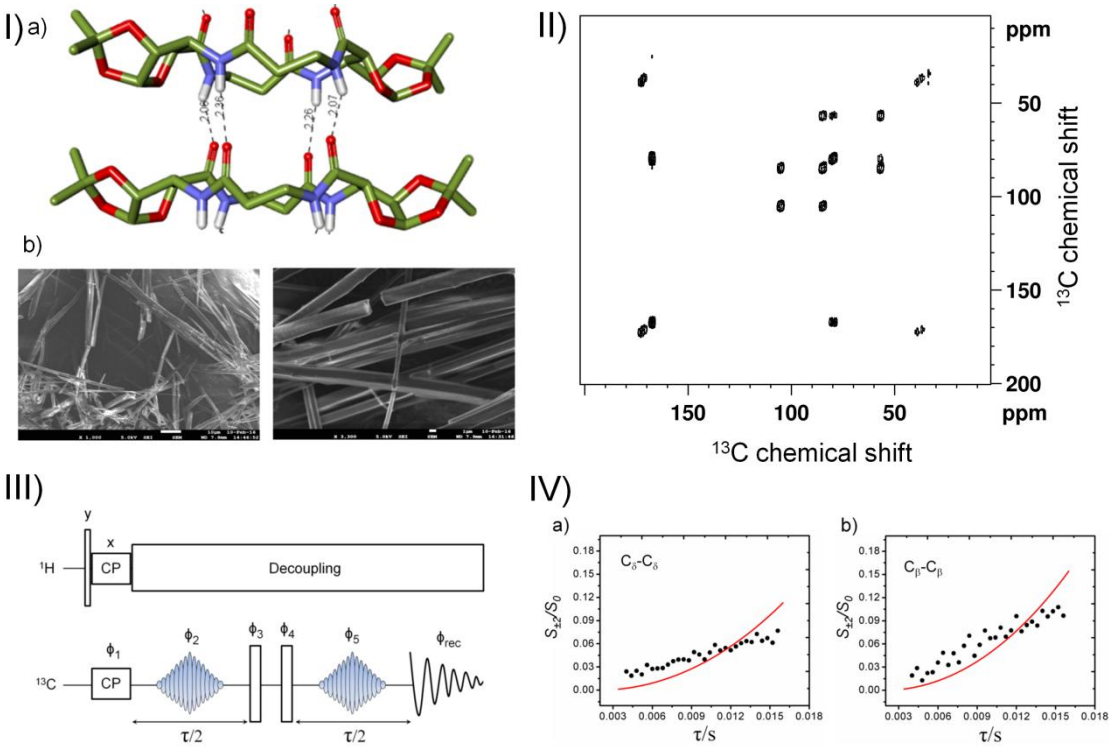

Figure 3: I) Density functional theory (DFT) calculated structures (a) and field emission scanning electron microscope (FE-SEM) images (b) of self-assembled cyclic-*β*-ASAS tetrapeptide. II) Solid-state NMR 2D-UC2QFCOSY (uniform-sign cross-peak double-quantum filtered correlation spectroscopy) spectrum of self-assembled ^{13}C, ^{15}N-labelled cyclic-β-ASAS tetrapeptide. III) Pulse sequence used for measuring selected internuclear ^{13}C–^{13}C dipolar couplings in self-assembled ^{13}C, ^{15}N-labelled cyclic-β-ASAS tetrapeptide. IV) Experimental amplitude ratio $S_{\pm 2}(\tau)/S_0(\tau)$ for ^{13}C nuclei in the C_δ (a) and C_β (b) sites of cis-β-fSAA in self-assembled ^{13}C, ^{15}N-labelled cyclic-β-ASAS tetrapeptide, plotted against the total delay, τ.

Chapter-5: The anisotropic environment of thermotropic liquid crystals is probed by using ^{129}Xe NMR spectroscopy. Pair-wise additive model is employed to account for the variation of ^{129}Xe nuclear shielding of the xenon gas dissolved in LC medium, as a function of temperature. The parameters such as ^{129}Xe shielding constant, the anisotropy of the shielding tensor, the temperature dependence of the isotropic shielding, and the shielding anisotropy, are derived. In conclusion, the present chapter explored the isotropic and anisotropic environments of the bulk and confined liquid crystals by recording ^{129}Xe nuclear shielding of xenon gas dissolved in the liquid crystal medium and the results are analyzed by using the *pair-wise additive* model.

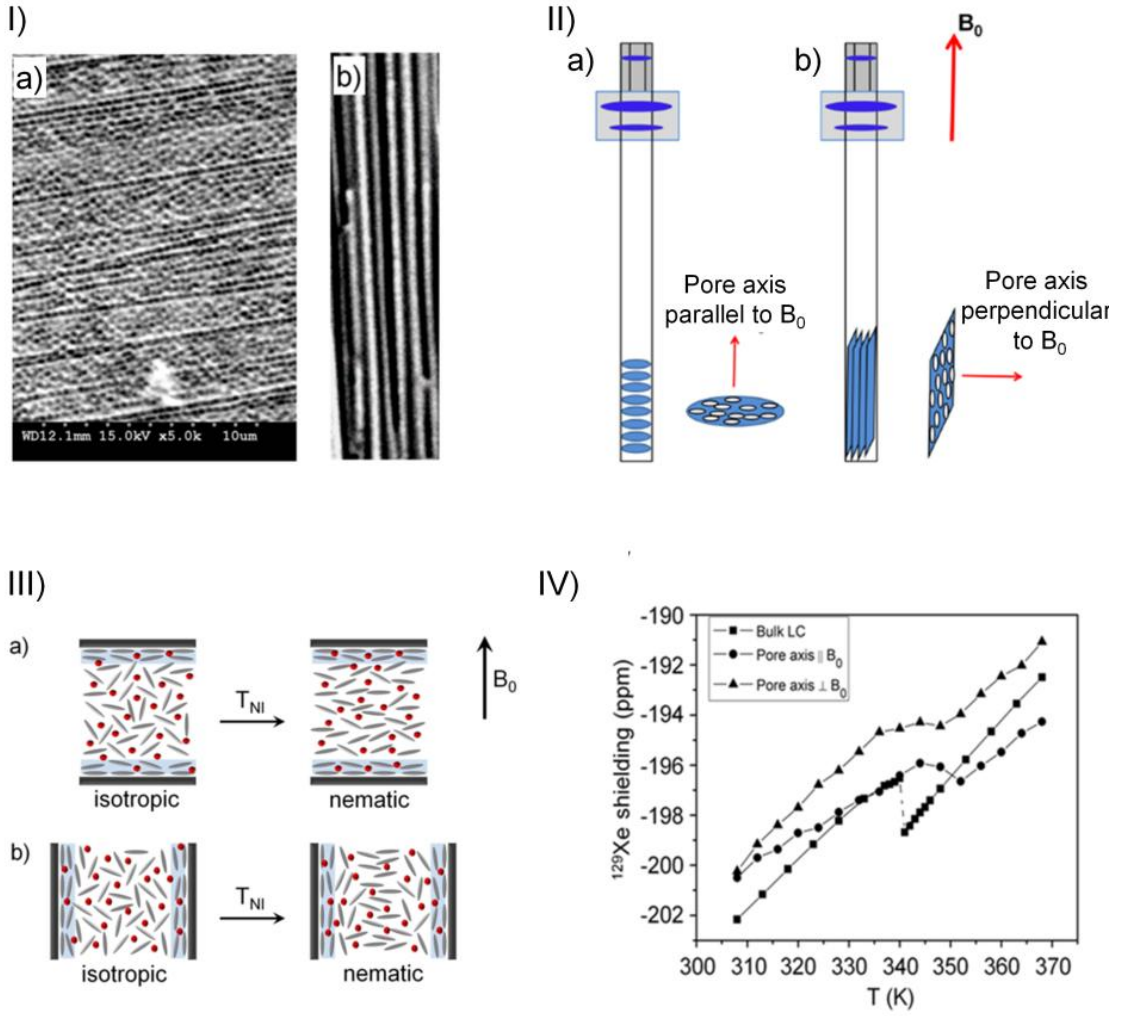

Figure 4: I) Scanning electron microscope (SEM) images of Anopore membranes: (a) surface and (b) cross-section. II) Experimental setup for the orientation of porous membranes (filled with liquid crystal) in magnetic field: (a) pore axis parallel to B_0 and (b) pore axis perpendicular to B_0. III) Schematic representation of the arrangement of liquid crystal molecules (⬭) and the occupancy of xenon atoms (●) in the isotropic and nematic phases of ZLI-1695 LC confined to cylindrical pores: (a) pore axis perpendicular to B_0 and (b) pore axis parallel to B_0. IV) ^{129}Xe chemical shifts of xenon gas dissolved in ZLI-1695 confined to cylindrical pores, as a function of temperature.